Front. Mech. Eng. 2022, 17(2): 26
https://doi.org/10.1007/s11465-022-0682-6

RESEARCH ARTICLE

Tribological study on the surface modification of metal-on-polymer bioimplants

Gang SHEN[a], Jufan ZHANG (✉)[a], David CULLITON[b], Ruslan MELENTIEV[a], Fengzhou FANG (✉)[a,c]

[a] *Centre of Micro/Nano Manufacturing Technology (MNMT-Dublin), School of Mechanical and Materials Engineering, University College Dublin, Dublin 4, Ireland*
[b] *Department of Aerospace, Mechanical and Electronic Engineering, Institute of Technology Carlow, Carlow, Ireland*
[c] *State Key Laboratory of Precision Measuring Technology and Instruments, Centre of Micro/Nano Manufacturing Technology (MNMT), Tianjin University, Tianjin 300072, China*

✉ *Corresponding author. E-mails: jufan.zhang@ucd.ie (Jufan ZHANG); fengzhou.fang@ucd.ie (Fengzhou FANG)*

ABSTRACT The tribological performance of artificial joints is regarded as the main factor of the lifespan of implanted prostheses. The relationship between surface roughness and coefficient of friction (COF) under dry and lubricated conditions is studied. Results show that under dry test, friction coefficient is not reduced all the time with a decrease in surface roughness. On the contrary, a threshold of roughness value is observed, and frictional force increases again below this value. This critical value lies between 40 and 100 nm in S_a (roughness). This phenomenon is due to the transfer of friction mechanisms from abrasion to adhesion. Under wet test, COF always decreases with reduction in surface roughness. This result is mainly attributed to the existence of a thin layer of lubricant film that prevents the intimate contact of two articulating surfaces, thus greatly alleviating adhesion friction. Furthermore, surface texturing technology is successful in improving the corresponding tribological performance by decreasing friction force and mitigating surface deterioration. The even-distribution mode of texturing patterns is most suitable for artificial joints. By obtaining the optimal surface roughness and applying texturing technology, the tribological performance of polymer-based bioimplants can be greatly enhanced.

KEYWORDS artificial joints, surface roughness, friction, surface texturing

1 Introduction

Total joint replacement (TJR) has been recognized as one of the most common surgical operations for decades [1–3]. It uses man-made joints to replace diseased natural bones so that patients could retain their daily life. Nowadays, the average lifespan of an artificial articular joint (AAJ) is approximately 15 years, which is too short for young patients to receive the TJR [4]. Moreover, such a short *in-vivo* service time leads to the need of revision operations, which negatively contributes to a huge economic effect. Referring to the data in Ref. [5], the mean cost of a revision operation is 76% more expensive than that of the corresponding primary arthroplasty. This high spending is a large burden for the national health care system and private savings. For example, between 1987 and 1993, Norway witnessed an annual cost of 1.7 million USD for the revision operation of artificial hip joints [6]. In addition, revision operation can cause severe physical damages to patients because a further cut of bones is needed to reshape the interface of the AAJ and the natural bones [7]. As a result, increase in the longevity of implanted joints can have economic and social benefits.

Many reasons explain why implant failure occurs after a specific *in-vivo* service time. Many researchers [8,9] reported that poor osseointergration could lead to an early failure of implanted joints. Some others concluded that fracture [10], displacement [11], and infections [12] can also negatively affect the longevity of artificial joints. The main trigger for the premature failure of implanted joints was widely reported to be the wear debris produced within the bearing surfaces [13]. More specifically, wear debris can have bioactive reactions with the surrounding bones and tissues, resulting in osteolysis [14]. In this case, aseptic loosening happens and subsequently, the

Received August 25, 2021; accepted February 28, 2022

implanted joints are not stably fixed, which would eventually contribute to the need for revision operations. Thus, ways to improve the tribological performance of implant bearing parts have become a popular research topic in the field of design and manufacture of AAJ. Shen et al. [15] conducted a comprehensive review on the methods to increase the longevity of bioimplants. The review presented that the modification of surface topography, including surface roughness and surface texturing, could improve the lubricating condition without sacrificing the mechanical properties of the bulk material. In the state-of-art, surface roughness is a major parameter affecting the tribological performance of any sliding system [16,17]. Technically, surface roughness is a parameter used to characterize the real components of a surface: peaks and troughs of different spacing, depths, and heights. When two bearing surfaces contact, the interaction between those peaks and troughs produce friction force or affect the tribological performance of bioimplants. A two-dimensional contact model was investigated by Ando and Ino [18] to correlate the relationship between asperity height and friction force. They found that friction force decreases with the decrease in asperity height, or friction force is reduced with the improvement in surface finish. This conclusion is consistent with many studies [19,20]. However, some scholars proposed that the situation would change when the bearing surfaces are polished to a mirror-like surface [21]. They found that the minimum friction force does not happen at the most polished surface, which is mainly due to the transfer of abrasive effect of surface asperities to adhesion forces when surface roughness is reduced. Molecular–mechanical theory of friction, which was published by Kragelskii [22], can explain this phenomenon. In the same decade, Bowden and Tabor developed conceptually similar adhesive-deformation theory of friction [23]. The main idea of both theories is that friction force is the sum of two components: the mechanical component representing the resistance of rubbing asperities to deformation and the molecular component standing for the formation and distraction of "cold-welded junction" in the regions of intimate contact between the counterparts. The idea allowed Coulomb theory of friction to be discarded and sourced the renaissance in our thinking about the behavior of rubbing solids, delivering Tribology Gold Medals to both developing parties in the 1980s. As far as the contribution of mechanical and molecular components to the friction force is proportional and inverse, respectively, to the size of surface irregularities, an equilibrium surface roughness provides the lowest coefficient of friction (COF) [22]. As a result, the identification of optimal surface roughness is a rational engineering step in designing any tribological system [24]. However, this step apparently has been ignored in some emerging tribological systems, including AAJ.

A very few studies took a challenge to reveal the optimal roughness conditions of cobalt–chromium–molybdenum (CoCrMo) and ultra-high-molecular-weight-polyethylene (UHMWPE) bearing counterparts of AAJ in corresponding kinematic and lubrication conditions. Both materials are hydrophilic in nature, which can increase the stability of lubricant film. The Young's modulus of UHMWPE (1.4 GPa) is more than two orders smaller than that of CoCrMo (210 GPa) [25]. Such design could make UHMWPE work as a soft cushion to adsorb vibrations produced during daily activities. The findings of most research works revealed that tribological performance is positively correlated to the surface roughness of bearing surfaces [20,26]. Moreover, in a hip simulator test, Wang et al. [27] proposed that no additional tribological benefits are achieved by further decreasing the roughness value below 20 nm in R_a (arithmetical mean height of a line). Weightman and Light [28] held a working hypothesis that the best tribological performance of UHMWPE-on-CoCrMo bioimplant does not happen at the finest surface finish, and surface roughness has a critical value. At a value smaller than this, tribological performance deteriorates again. However, they failed to find this optimum value. Since then, the idea of finding the optimum roughness value has been absent, and no explanation has been made on whether such value exists for the bioimplant area. However, the idea that the best tribological performance does not happen at the finest surface finish has been proven in other areas. Feng et al. [29] investigated the friction performance of rubber elastomers and found that the minimum COF occurs when counter face roughness is between 30 and 85 nm in R_a. Brinksmeier et al. [21] obtained a similar conclusion in the steel-on-steel articulating system, where the lowest COF happens when the S_a (arithmetical mean height) value ranges between 200 and 400 nm. Both systems work under the dry condition, which is different from that of the bioimplant. To check whether the working environment affects the optimum roughness for a specific material combination, the dry test of CoCrMo-on-UHMWPE will be carried out in this paper.

In general, a good design of the optimal surface roughness only reduces asperity interactions between bearing surfaces. However, the thickness of the lubricant film cannot increase greatly by only obtaining the optimal surface roughness. Furthermore, considering the long-term *in-vivo* service time of implanted joints, this issue is more profound for the orthopedic industry [30]. Surface texturing technology was widely discussed in the literature to affect the tribological performance of different applications [15,25,31–33]. As for bioimplants, Choudhury et al. [34] confirmed that texturing patterns improve the lubricating effect by forming a thicker film in the vicinity of micro dimples. Much effort has been devoted to measuring the friction and wear directly after applying texturing technology. Ito et al. [35] found that

fabricating micro dimples (500 μm diameter, 1200 μm pitch distance, and 100 μm depth) on the bearing surface of CoCrMo reduced the wear loss of UHMWPE by 69%. An improvement in the tribological performance of dimple-textured bioimplants was also reported in Refs. [13,36,37]. Shen et al. [25] comprehensively studied the role of five pattern parameters, namely, pattern shape, size, area density, depth, and distribution mode. They found that the triangle pattern with 200 μm side length, 10% area density, 8–10 μm depth, and square-array distribution mode can provide the best tribological performance. Although most scholars agree that surface texturing can increase the tribological performance of polymer-based bioimplants, the working mechanism behind this phenomenon remains missing. One of our previously published review papers [15] revealed four possible working mechanisms: (1) trapping hard particles, (2) increasing wettability, (3) providing hydrodynamic pressure, and (4) reserving lubricants. The first two working mechanisms are widely accepted in the state-of-art because trapping hard particles can reduce the occurrence of three-body abrasive wear [38], whereas increased wettability can help form a more stable lubricant film [39]. However, scholars have different views regarding how surface texturing can help promote load-carrying capacity. Many researchers claimed that hydrodynamic pressure induced by micro patterns should be the main source to form thicker lubricant film [40–42], whereas some scholars opposed this idea, claiming that low viscosity and slow velocity working condition made hydrodynamic pressure played a minor role in the tribological performance of textured bioimplants [43,44]. Although scholars have different views regarding which pattern parameter can provide the best tribological performance or which working mechanism plays the main role, one common feature of texturing investigation is in the state-of-art: The pitch distance between any two adjacent patterns is constant in one bearing surface [37,45,46]. In another word, micro patterns are evenly distributed on the contact surface. However, no study confirmed that the tribological performance of evenly distributed patterns is better than that of unevenly distributed patterns. Furthermore, the scanning electron microscope (SEM) image of the natural articular surface shows that micro dimples are unevenly distributed on the bearing area [47]. Inspired by this natural feature, Melentiev and Fang [48] used sandblasting technology to modify the bearing surface of CoCrMo, making it similar to that of natural joints, but they did not conduct any tribological investigation. Hence, knowledge regarding which distribution mode is suitable for bioimplants remains lacking.

Two surface features of CoCrMo will be studied in this paper to improve the tribological performance of implanted joints. First, molecular–mechanical friction theory will be checked in the CoCrMo-UHMWPE material combination. Hence, the optimal S_a value will identify where the COF goes through the point of extremum (minimum) in dry and serum-lubricated conditions so that tips can be provided on whether working condition will influence the application of molecular–mechanical friction theory. Second, surface texturing technology will be applied based on the optimal surface roughness to improve the corresponding lubricating condition further. More specifically, the distribution mode of texturing patterns will be discussed to obtain the best tribological performance. This paper can provide tips for relevant practitioners in the orthopedic area to design bioimplants with better tribological performance.

2 Experimental approaches

2.1 Preparation and characterization of bearing surface with various roughness values

Lapping and polishing were used in treating the bearing surfaces of CoCrMo disks. The disk was 30 mm in diameter and 10 mm in height, which provided a bearing area similar to that of implanted hip joints [30]. Sandpapers with grit numbers of 180, 240, 320, 600, 1200, and 2500 were adopted for lapping, and suspensions of 3 μm diamond and 40 nm colloidal silica were used to decrease the surface roughness of the metallic samples further. A large range of roughness values was achieved, and the corresponding data were evaluated using NPFLEX white light interferometry (WLI, Bruker). Each sample was measured 10 times using the vertical scanning interferometry mode, and the sampling area was 2.4 mm × 3.2 mm. S_a (arithmetical mean height) was used to characterize the surface roughness of the bearing surfaces. A smaller sampling area (66 μm × 88 μm) was also adopted to present more detailed 3D information of how peaks and troughs are distributed on the bearing surface. SEM and optical microscope (Keyence) were used to measure surface morphology and worn tracks.

2.2 Surface texturing

Micro-abrasive jet machining (MAJM) was used to fabricate micro dimples on the CoCrMo bearing surface (refer to Refs. [30,49]). In MAJM, pressurized air (0.4 MPa) was used to speed up micro particles through a needle-like nozzle with 0.5 mm diameter. In this paper, the micro particle was alumina with an equivalent diameter of 28 μm. The angle between the micro nozzle and the CoCrMo disk was 90°, and the distance between the nozzle's end surface and the disk was 1 mm. To fabricate designed micro patterns with a square-like floor profile, 0.1 s was the manufacturing time for each micro dimple. Afterward, textured disks were lapped and

polished to obtain the optimal surface roughness for the bearing area.

2.3 Pin-on-disk tester

To establish the relationship between surface roughness and COF as well as confirm which distribution mode is most suitable for the CoCrMo-UHMWPE bearing system, a pin-on-disk tribometer (NFW120, NEOPLUS) was used. In this instrument, a high-accuracy load cell with a resolution of 6 mN was used to achieve precise friction measurement. The pin was held still while the disk was rotated at a constant speed (see Fig. 1). The pin was specifically shaped as a stepped cylinder with 2 mm diameter of articulating surface. This pin structure was designed to eliminate misalignment, and several pilot experiments showed that the contact surfaces were worn homogeneously. Moreover, the pins were machined from UHMWPE cuboid (GUR 1020), and the material combination in this paper (CoCrMo-UHMWPE) is consistent with previous studies of other researchers [50,51]. Sliding speed was set as 40 mm/s and kept constant during the tests. Applied load was 10 N, which provided a 3.18 MPa contact pressure [52]. To simulate the property of synovial fluid encountered by implanted joints, a proper solution was selected for *in-vitro* experiments. Some scholars comprehensively studied the role of different components of the synovial fluid in the formation of lubricant film and confirmed that bovine serum can be used as a replacement of synovial fluid in laboratory tests [53–56]. Hence, for the wet tests in this paper, bovine serum (B9433, Sigma-Aldrich) was used as the lubricant. It was diluted to 25% (v/v) with deionized water to simulate the mechanical properties of synovial fluid, which has a viscosity value of 0.023 Pa·s. A certain amount of solution (140 mL) was used to achieve a flooded lubricating condition. The pilot studies showed that the running-up period only lasted for dozens of seconds. Thus, a 10-minute experiment was carried out for all surfaces, which provided a 24-meter sliding distance. The friction measurement for each sample was repeated at least twice to alleviate random error. All samples were cleaned thoroughly before the friction tests. Here, the pin and disk samples were first rinsed with tap water for 30 s and then cleaned with deionized water in an ultrasonic cleaner for 6 min. Next, all samples were rinsed with ethanol and then dried with pressurized airflow.

3 Correlation between surface roughness and COF

3.1 Surface topography

The surface topographies of tested samples are shown in Fig. 2. The finest surface finish achieved in this paper was 8.6 nm in S_a, which is comparable to the smallest S_a value for commercial products and academic research. Some rougher surfaces were used to provide a more elaborate correlation between surface roughness and COF. Surfaces with various roughness exhibited remarkably different morphology patterns. The topography obtained with #180 sandpaper (see Fig. 2(a)), was teeming with sharp peaks, crests, and ridges, the highest of which could reach 2.2 μm. Protruding parts were also presented on some other samples (Figs. 2(b) and 2(c)), but their amplitudes were twofold and fourfold smaller than that in Fig. 2(a), respectively. As a result, due to this common feature, these three bearing samples were grouped as peak-rich surface. However, the profile topography showed no evident protruding asperities in Figs. 2(d) and 2(e). In terms of finely polished samples, it

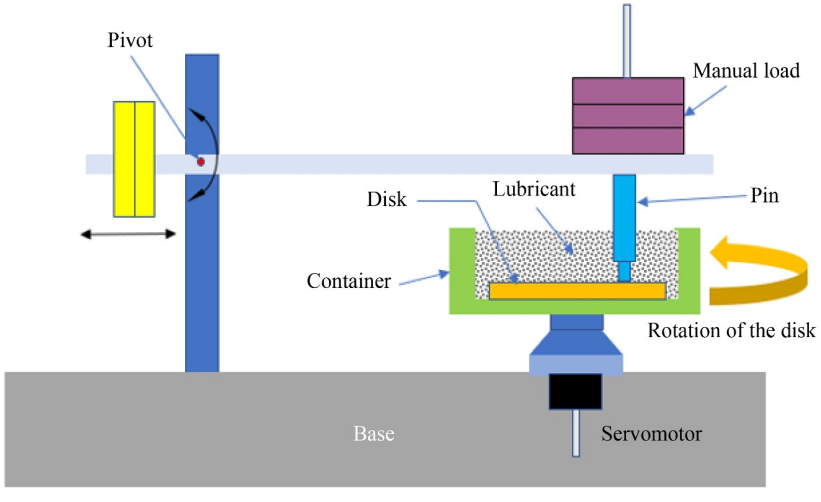

Fig. 1 Schematic illustration of pin-on-disk tribometer.

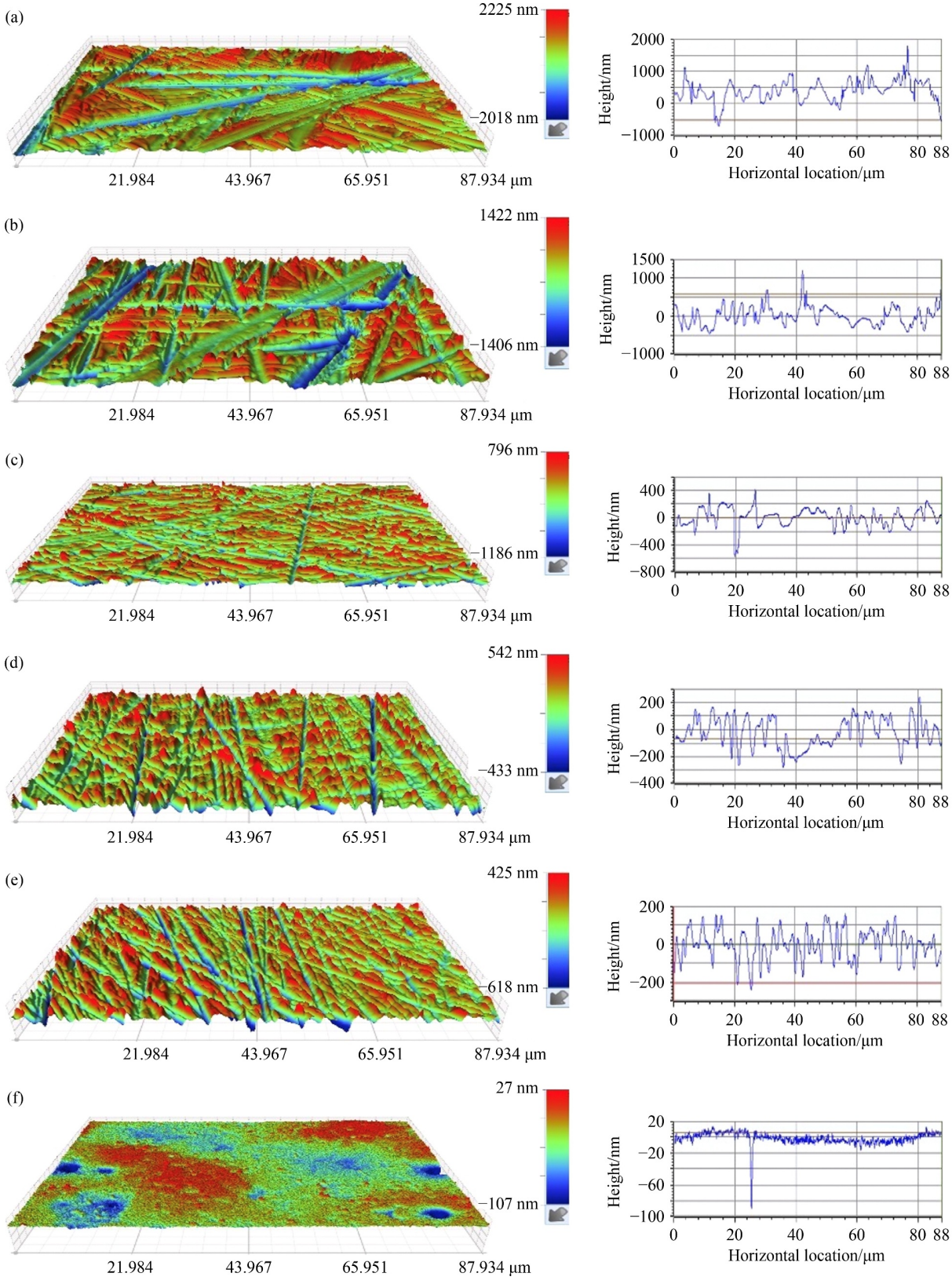

Fig. 2 Surface topography of CoCrMo samples with various roughness values (S_a): (a) 337.4 nm, (b) 184.8 nm, (c) 98.4 nm, (d) 60.6 nm, (e) 48.2 nm, and (f) 8.6 nm.

had a nanoscale surface finish with sparse but relatively deep pits on its bearing face. Alternatively, these three samples were grouped as plateau-like surface. The difference in surface topography can be further seen in

Fig. 3. Samples' surfaces with a lower S_a value had a less inclined bearing curve, which represents a transfer of surface topography from peak-rich to plateau-like surface. Peak-rich topographies had notable larger areas of the first contact and void areas. It signifies that the bearing area is relatively small compared with plateau-like topographies. Therefore, the latter group implies a lower level of mechanical interlocking of frictional counterparts, particularly at the initial stage of friction test, and suggests better conditions for uniform pressure distribution within the contact spot.

3.2 Coefficient of friction (COF) under dry test

Figure 4 shows COF versus surface roughness in CoCrMo-UHMWPE pin-on-disk test under dry conditions. The COF demonstrated a statistically significant and distinctive dependency on roughness parameter of S_a. The best fit was achieved with a polynomial regression curve, having the coefficient of determination R^2 = 0.9017. The roughest surfaces, with the S_a value of around 337 nm, showed quiet large frictional values, which ranged between 0.35 and 0.4. When the bearing was finely polished to a mirror surface, its roughness value was reduced to below 10 nm. The COF for the mirror-like surface decreased to approximately 0.2, which was about half of that when polymer pin slided against the roughest CoCrMo disk in this paper. However, the lowest COF did not happen where bearing surface was finely polished. Alternatively, articulating bearings, with surface roughness of about 48 and 60 nm in S_a, both had smaller COF values than mirror surfaces. The trend in Fig. 4 clearly shows a critical roughness value where the smallest COF exists, and when surface roughness is smaller than this critical value, COF increases again. From a practical point of view, achieving an optimal working condition is more useful where a system exhibits the best performance. Thus, for CoCrMo-UHMWPE material combination under dry sliding, the optimal roughness range with the lowest COF was between 40 and 100 nm. Any surface with S_a value larger than 100 nm or smaller than 40 nm would have a worse tribological performance.

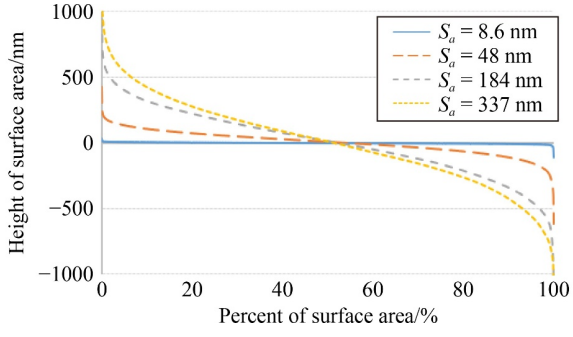

Fig. 3 Bearing behavior of testing samples.

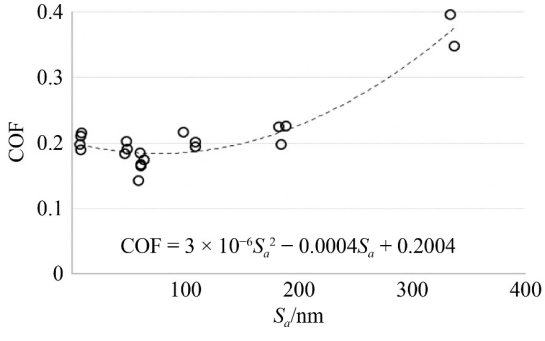

Fig. 4 COF vs. S_a under dry test.

To elaborate the reason behind this nonlinear trendline explicitly, the mechanisms of how friction is produced with surfaces under different roughness values need to be investigated. Figure 5 shows the surface morphologies of worn UHMWPE when sliding against CoCrMo with different S_a values. When the counter face was the peak-rich surface, many scratches were on the polymer bearings (refer to Figs. 5(a) and 5(b)). These deep scratches were caused by the abrasive effect of protruding asperities on the CoCrMo surfaces. Such finding was also observed by some other scholars. Lancaster [57] found that the cutting effect of sharp peaks is the main phenomenon for polymer material when its counter face is rougher. A similar study was done by Xie and Williams [58] using hard-on-soft material combination, and they concluded that hard surfaces with higher asperities are prone to cutting or ploughing soft surfaces. However, when samples are smoother, bearing surfaces became more plateau-like. This kind of surface provides a platform where asperities on UHMWPE bearing could have an intimate contact (atomic level) with its metal counterpart [59]. As a result, micro junctions are formed, and atomic force plays the main role in binding these two materials. Owing to cyclic motion, these micro junctions rupture, and polyethylene adheres to the metallic bearing surface. In Figs. 5(c) and 5(d), no scratches were seen the surfaces, but the adhesion effect could be seen clearly. As a result, adhesion force was the predominant mechanism for the friction force when sliding against the plateau-like surface. The explanation above was further proven by the worn samples (refer to Fig. 6). When the CoCrMo disk was rough, its polymer counterpart was scratched by the protruding asperities, and then wear debris accumulated around the deep valleys. However, due to the intimate contact between the polymer asperities and the flat disk, lumps of UHMWPE adhered on its counter face.

In summary, under dry testing conditions, COF first decreases with a decrease in surface roughness and then increases when surface finish is further improved. The optimal working roughness range is between 40 and 100 nm for the CoCrMo-UHMWPE combination. Moreover, the result is consistent with the theoretical model provided by Kragelskii [22], which means, under dry test, friction

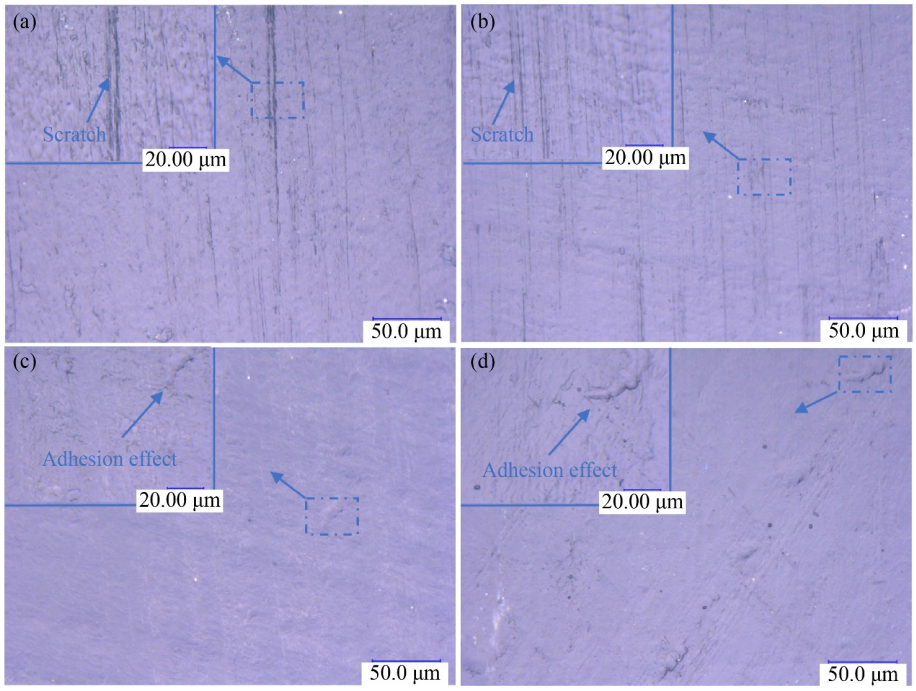

Fig. 5 Worn surfaces of UHMWPE when sliding against CoCrMo with different surface roughness values (S_a): (a) 337 nm, (b) 184 nm, (c) 48 nm, and (d) 8.6 nm.

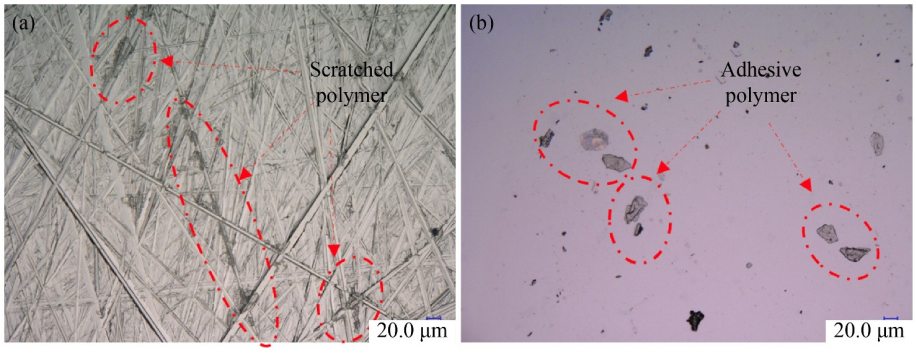

Fig. 6 Worn metal samples with S_a values: (a) 337 nm and (b) 8 nm.

mainly consists of two components: mechanical part (abrasive effect of protruding asperities) and molecular part (adhesive force). The effect of mechanical component decreases with the surface roughness, and no mechanical component exists when the surface is perfectly smooth. The molecular component is weak when the metallic bearing surface is rough, and it has a stronger effect with smoother surface finish. Thus, with the decrease of surface roughness, friction mechanisms transfer from abrasion (mechanical component) to adhesion (molecular component), and the sum of these two components contributes to the trendline found in this paper.

3.3 Coefficient of friction under serum-lubricated condition

Figure 7 shows the test results under serum-lubricated condition. This trendline, with a coefficient of determination R^2 of 0.9266, is different from that derived under dry test. Here, COF decreases almost linearly with surface roughness. The surface roughness of finely polished samples used for the serum-lubricated tests is between 7 and 10 nm in S_a, and Fig. 7 shows it is the roughness value where the minimum COF exists. However, some scholars experimentally evaluated the wear properties of polymer-based joints and reported that improving the surface finish of metallic surfaces below 20 nm in R_a is not needed [27]. Lancaster et al. [26] also reported that the roughness of clinical implants is between 5 and 40 nm in R_a. Even for the regulations in ISO 7206-2:2011 and ISO 7207-2:2011, the surface roughness of hip and knee articulating surfaces should be smaller than 2 μm when applying 0.08 mm short wavelength cut-off, which was also adopted to treat the

surface roughness in this paper. However, based on the finding of this work, the CoCrMo articulating surface must have an average S_a value smaller than 10 nm. Furthermore, CoCrMo surfaces with an average S_a below 5 nm do not need polishing. The manufacturing costs and difficulty in achieving such a surface finish are currently, unacceptable. The reduction rates in COF when surface roughness is reduced from 10 nm to even 5 nm or even 1 nm are 1.8% and 3.4%, respectively.

In terms of friction mechanisms, under dry tests, the transfer of abrasion to adhesion results in the increase of COF when surface roughness is smaller than a critical value. As reported by Affatato [59], intimate contact (atomic scale) between two bearing surfaces is the essential requirement for adhesion wear, and if a layer of lubrication film is between the bearings, the chance for adhesion is greatly reduced. A layer of noncontinuous lubricating film is between two articulating surfaces, although its thickness varies among different research [4,41,60]. Hence, the CoCrMo-UHMWPE bearing system works under a situation between boundary and mixed lubrication [30]. With a decrease in surface roughness, the bearing system works under a condition closer to the mixed lubrication. In this case, adhesion is less likely for plateau-like surfaces under serum-lubricated conditions. The difference of frictional performance between dry test and serum-lubricated condition is clearly seen in Fig. 8. First, the COF of the wet test is always smaller than that under dry condition because the lubricating film reduces the asperity contacts of two bearings. Furthermore, the existing lubricant film alleviates the effects of adhesion friction force when the surface roughness is very low. As a result, its COF is reduced almost linearly with surface roughness, which is different from that under dry test.

In summary, molecular–mechanical friction theory can only be applied to the sliding system with no lubricant film between the contact surfaces, and an optimal roughness value exists when the minimum COF can be obtained. As for CoCrMo-UHMWPE bioimplant, synovial fluids exist within contact surfaces, which means molecular friction plays a minor role in implanted joints. To achieve the best tribological performance, the S_a of the CoCrMo bearing part should be smaller than 10 nm.

As stated in published review works [52], the sliding velocity and applied loading used in this paper are similar to those of implanted joints. Furthermore, because the properties of diluted bovine serum bear a great similarity to that of synovial fluids [61], the testing conditions in this paper could be regarded as a simplified *in-vivo* environment. Thus, the trendline derived under the serum-lubricated test could provide us some insights into designing and fabricating artificial joints. As discussed above, to achieve a long *in-vivo* service time, CoCrMo surfaces must be polished to have as S_a value smaller than 10 nm. However, only polishing the CoCrMo surfaces as

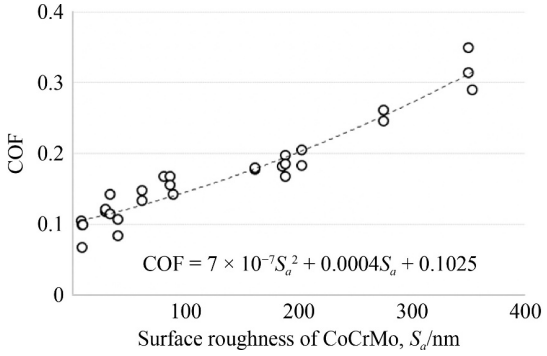

Fig. 7 COF vs. surface roughness under serum-lubricated condition.

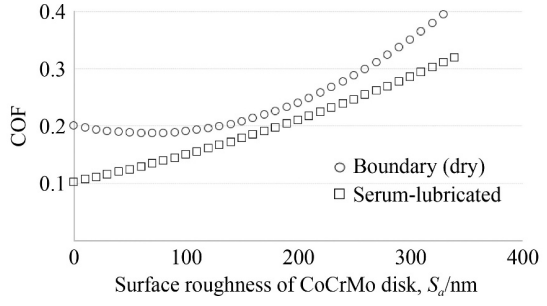

Fig. 8 Comparison of COF between dry test and serum-lubricated condition.

smooth as possible is not sufficient. Maintaining that initial level of roughness is more important. Studies frequently reported that metallic articulating surfaces become rough during *in-vivo* service, which is mainly due to three-body abrasion caused by hard particles [62,63]. Figure 9 shows many scratches on the CoCrMo disk only after 10-minute sliding, causing the roughening of articulating surfaces. In this case, COF increases with implantation time. For instance, when surface roughness is only 30 nm, the friction coefficient is around 0.115, which is 8% larger than that of finely polished samples. As a result, to achieve a long-term tribological performance, some methods must be adopted to prevent the deterioration of metallic surface roughness. As discussed in the Introduction section, fabricating micro patterns on the CoCrMo bearing surface can well trap the hard particles. Hence, this technology will be discussed in the next section to see how it can help improve the tribological performance of bioimplants.

4 Effect of texturing patterns

After MAJM, the bearing surface of the textured CoCrMo disk is deteriorated by the abrasive effect of alumina particles (refer to Fig. 10). After MAJM, the texturing pattern is a micro dimple with diameter of 600 μm and depth of 6 μm. The average S_a value of bearing area in

Fig. 9 SEM image of CoCr surface after 10-minute wear under serum-lubricated situation.

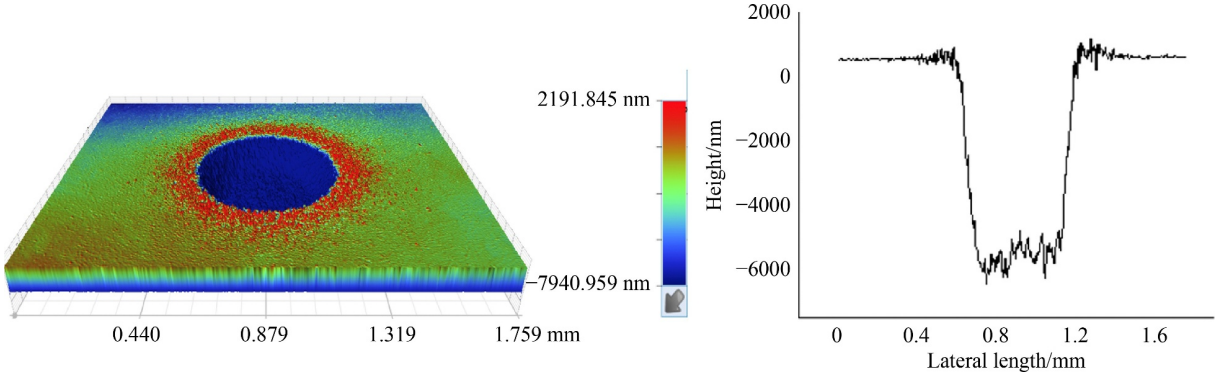

Fig. 10 WLI image of micro dimple after MAJM.

the vicinity of micro patterns is around 150 nm, which is much larger than the optimal roughness value found in the previous section. A more devastating situation is that some protruding asperities (bulges) are near the micro dimple, and their height can reach nearly 1 µm. These sharp peaks work as abrasive tools after being implanted into the human body [30]. All textured surfaces were lapped and then polished to achieve the desired surface finish (S_a < 10 nm) due to these two reasons. Figure 11 shows that a superfine surface roughness is achieved, and no protruding asperities can be found on the bearing surface. Moreover, after the post-treatment, the top diameter of the circular pattern is reduced from the original 600 to 550 µm. The depth is decreased by 1 to 5 µm after the final polishing procedure.

The three distribution modes of dimple patterns are shown in Fig. 12. In Fig. 12(a), the conventional even-distribution mode is exhibited (namely, D1), where the pitch distance is constantly 2 mm. In this case, the area density of the texturing patterns in D1 is around 6%. Two uneven distribution modes are studied in this section while the area densities are both kept as 6%. Figure 12(b) (namely, D2) shows that the pitch distance is either 1 or 3 mm. Although the overall area density in D2 is 6%, the texturing density in some local areas can be as high as 24%. A more extreme distribution mode of micro dimples can be seen in Fig. 12(c) (namely, D3). Here, the pitch distance between two adjacent patterns is either 0.8 or 3.2 mm. In this case, the density of texturing patterns in some local areas of D3 can reach 37%.

The frictional performance of dimple-textured samples under three distribution modes is exhibited in Fig. 13. When micro patterns are evenly distributed on the bearing surfaces (D1), it holds the smallest COF (0.0782) among the three samples. As for the textured surfaces with uneven distribution form, both samples have larger COF values than D1. The COF of D2 is 0.0895, which is 14.5% larger than that of D1. In terms of the more extreme distribution form (D3), its COF value reaches 0.0979, which is 25.2% larger than that of D1. Moreover, referring to the model in Fig. 7, the COF is about 0.1065 when the CoCrMo disk has an S_a value of 10 nm. Hence,

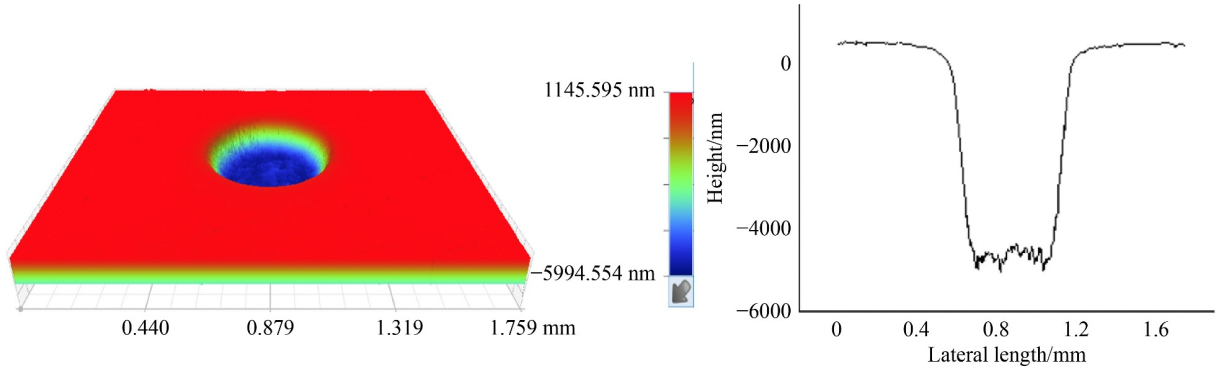

Fig. 11 WLI image of micro dimple after lapping and polishing.

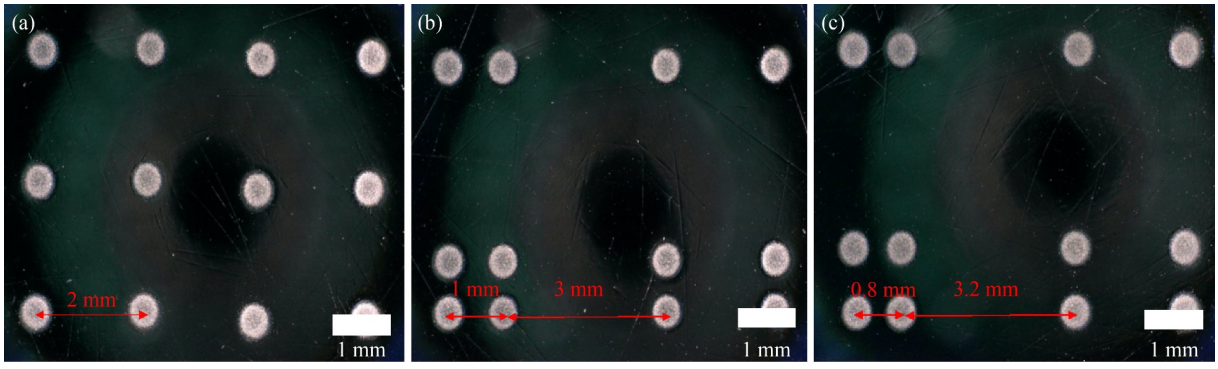

Fig. 12 Optimal images of three distribution modes for micro dimple: (a) even distribution, and the pitch distance is constantly 2 mm (namely, D1); (b) uneven distribution mode 1, and the pitch distance can be either 1 or 3 mm (namely, D2); (c) uneven distribution mode 2, and the pitch distance can be either 0.8 or 3.2 mm (namely, D3).

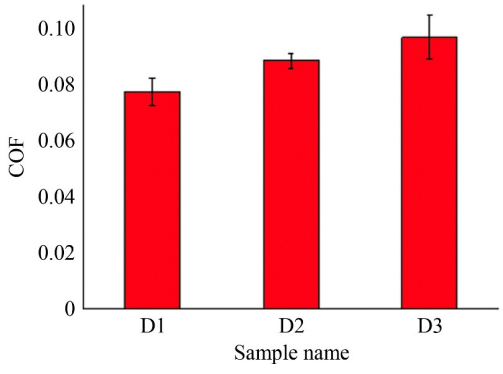

Fig. 13 COF of dimple-textured CoCrMo disks under three different distribution modes.

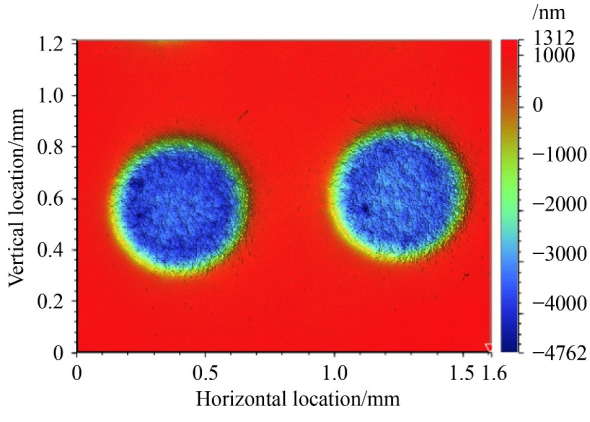

Fig. 14 CoCrMo bearing surface after pin-on-disk sliding test.

the textured samples under all three distribution modes exhibit better tribological performance than only polished samples. Furthermore, the even distribution mode is most suitable for the textured CoCrMo-UHMWPE bioimplant. Other than the improved frictional performance, no evident micro scratches such as those on the polished surface can be found on the bearing surface of CoCrMo disk after applying texturing technology (see Fig. 14). Hence, the limit of only controlling surface roughness before implantation is solved by using texturing technology.

The reason why the even-distribution mode of texturing patterns is most suitable for bioimplants can be easily answered by theory published in our previously published paper [30]. The deformation of the polymer part can squeeze out the reserved fluids inside micro patterns. In this manner, a thicker lubricant film is formed in the vicinity of micro patterns to separate the bearing surfaces [64]. However, the interlocking effect is more likely with the increase of area density. Interlocking effect means that the edge of micro patterns can scratch the polymer

counterpart offering the additional two-body abrasion friction force. Given that the local area density in D2 and D3 can be as high as 24% and 37%, respectively, the positive tribological performance offered by surface texturing is mitigated by the interlocking effect. Furthermore, the extra abrasion friction force is larger in samples with higher local area density, which is consistent with the finding in this paper.

The conclusion in this part is of great importance for the application of surface texturing in the field of bioimplants. First, it shows that finding some fabricating technologies to replicate the micro patterns of natural articular surfaces on artificial joints is not meaningful. Second, it proves the need to control the position of each micro pattern precisely on the bearing surfaces of artificial joints so that pitch distance is constant between any two adjacent patterns. Considering the difficulty in manufacturing micro patterns on the freeform surface of knee joints and the need for post-treatment of bearing surfaces, manufacturing micro patterns on the bearing surfaces of bioimplants is currently very difficult and expensive. Hence, current texturing techniques should be greatly modified, or novel texturing techniques should be proposed for mass production in the future.

5 Conclusions

A tribological study on the surface modification of CoCrMo-on-UHMWPE material combination was conducted. First, molecular–mechanical friction theory was checked under dry and serum-lubricated conditions. Second, surface texturing technology was investigated to solve the limits of only controlling the surface roughness of bearing surfaces.

Under dry working conditions, molecular–mechanical friction theory can be applied in the target material couple. The smoothest surface does not provide the smallest COF. Alternatively, the optimal working range of S_a for the CoCrMo-UHMWPE system, where best tribological performance exists, is between 40 and 100 nm. This trendline is caused by the transfer of friction mechanisms from the mechanical part (abrasive effect of protruding asperities) to the molecular part (adhesive force).

As for serum-lubricated condition, COF decreases with a decrease in surface roughness. The molecular component of friction force plays a minor role between the two contact surfaces due to the existence of the lubricant film. Moreover, from a practical point of view, the CoCrMo bearing surface must be polished to have a S_a value smaller than 10 nm. Furthermore, only obtaining the optimal surface roughness is not sufficient to ensuring a good long-term tribological performance because surface deterioration (micro scratches) occurs on CoCrMo after experiencing relative motion.

Finally, surface texturing technology improves the tribological performance of the CoCrMo-UHMWPE bearing system under serum-lubricated conditions in two aspects: (1) COF decreases compared with only polished samples, and (2) no surface deterioration is observed on metal bearing surfaces. Moreover, the even-distribution mode of texturing patterns is most suitable for the CoCrMo-UHMWPE bearing couple. In summary, after obtaining the optimal surface roughness and applying surface texturing technology, the corresponding tribological performance can be greatly improved.

Given the limits that pin-on-disk testing cannot provide same working condition as that encountered by implanted joints, future work will be done to test the tribological performance of surface-modified bioimplants using sophisticated hip or knee simulators. Furthermore, the role of different components of the synovial fluid in the formation of lubricant film will be studied to provide more detailed working mechanism for surface-structured bioimplants.

Acknowledgements This publication emanated from research conducted with the financial support of the Science Foundation Ireland (Grant No. 15/RP/B3208). For the purpose of Open Access, the author has applied a CC BY public copyright license to any Author Accepted Manuscript version arising from this submission. The “111” Project by the State Administration of Foreign Experts Affairs and the Ministry of Education of China (Grant No. B07014) is also acknowledged. The authors appreciate the help provided by the Extreme Optoelectromechanix Laboratory of the East China Normal University in fabricating micro patterns. Acknowledgments are extended to Orthoplastics for providing UHMWPE materials and Beijing Jinzhi Hongtai Metal for providing CoCrMo disks. Open Access funding provided by the IReL Consortium.

References

1. Kang C W, Fang F Z. State of the art of bioimplants manufacturing: part I. Advances in Manufacturing, 2018, 6(1): 20–40
2. Wang Z W, Yan Y, Wang Y, Su Y J, Qiao L J. Lifecycle of cobalt-based alloy for artificial joints: from bulk material to nanoparticles and ions due to bio-tribocorrosion. Journal of Materials Science & Technology, 2020, 46: 98–106

3. Cui W, Bian Y Y, Zeng H K, Zhang X G, Zhang Y L, Weng X S, Xin S X, Jin Z M. Structural and tribological characteristics of ultra-low-wear polyethylene as artificial joint materials. Journal of the Mechanical Behavior of Biomedical Materials, 2020, 104: 103629
4. Jin Z M, Dowson D, Fisher J. Analysis of fluid film lubrication in artificial hip joint replacements with surfaces of high elastic modulus. Proceedings of the Institution of Mechanical Engineers, Part H: Journal of Engineering in Medicine, 1997, 211(3): 247–256
5. Weber M, Renkawitz T, Voellner F, Craiovan B, Greimel F, Worlicek M, Grifka J, Benditz A. Revision surgery in total joint replacement is cost-intensive. BioMed Research International, 2018, 2018: 8987104
6. Furnes A, Lie S A, Havelin L I, Engesaeters L B, Vollset S E. The economic impact of failures in total hip replacement surgery: 28,997 cases from the Norwegian arthroplasty register, 1987–1993. Acta Orthopaedica Scandinavica, 1996, 67(2): 115–121
7. Revision Total Hip Replacement. Available from American Academy of Orthopaedic Surgeons website. Accessed on June 2021
8. Albrektsson T, Brånemark P I, Hansson H A, Lindström J. Osseointegrated titanium implants: requirements for ensuring a long-lasting, direct bone-to-implant anchorage in man. Acta Orthopaedica Scandinavica, 1981, 52(2): 155–170
9. Willmann G. Improving bearing surfaces of artificial joints. Advanced Engineering Materials, 2001, 3(3): 135–141
10. Hwang D S, Kim Y M, Lee C H. Alumina femoral head fracture in uncemented total hip arthroplasty with a ceramic sandwich cup. The Journal of Arthroplasty, 2007, 22(3): 468–471
11. Nevelos J, Ingham E, Doyle C, Streicher R, Nevelos A, Walter W, Fisher J. Microseparation of the centers of alumina-alumina artificial hip joints during simulator testing produces clinically relevant wear rates and patterns. The Journal of Arthroplasty, 2000, 15(6): 793–795
12. Fitzgerald R H Jr. Infections of hip prostheses and artificial joints. Infectious Disease Clinics of North America, 1989, 3(2): 329–338
13. Sawano H, Warisawa S, Ishihara S. Study on long life of artificial joints by investigating optimal sliding surface geometry for improvement in wear resistance. Precision Engineering, 2009, 33(4): 492–498
14. Lombardi A V Jr, Mallory T H, Vaughn B K, Drouillard P. Aseptic loosening in total hip arthroplasty secondary to osteolysis induced by wear debris from titanium-alloy modular femoral heads. The Journal of Bone and Joint Surgery. American Volume, 1989, 71(9): 1337–1342
15. Shen G, Fang F Z, Kang C W. Tribological performance of bioimplants: a comprehensive review. Nanotechnology and Precision Engineering, 2018, 1(2): 107–122
16. Melentiev R, Kang C W, Shen G, Fang F Z. Study on surface roughness generated by micro-blasting on Co-Cr-Mo bio-implant. Wear, 2019, 428–429: 111-126
17. O'Toole L, Kang C W, Fang F Z. Advances in rotary ultrasonic-assisted machining. Nanomanufacturing and Metrology, 2020, 3(1): 1–25
18. Ando Y, Ino J. The effect of asperity array geometry on friction and pull-off force. Journal of Tribology, 1997, 119(4): 781–787
19. Wong H C, Umehara N, Kato K. The effect of surface roughness on friction of ceramics sliding in water. Wear, 1998, 218(2): 237–243
20. Svahn F, Kassman-Rudolphi Å, Wallén E. The influence of surface roughness on friction and wear of machine element coatings. Wear, 2003, 254(11): 1092–1098
21. Brinksmeier E, Riemer O, Twardy S. Tribological behavior of micro structured surfaces for micro forming tools. International Journal of Machine Tools and Manufacture, 2010, 50(4): 425–430
22. Kragelskii I V. From the editorial board. Journal of Friction and Wear, 2008, 29(3): 164–170
23. Field J. David Tabor. 23 October 1913–26 November 2005. Biographical Memoirs of Fellows of the Royal Society, 2008, 54: 425–459
24. Kragelsky I V, Dobychin M N, Kombalov V S. Friction and Wear: Calculation Methods. New York: Pergamon Press, 1982
25. Shen G, Zhang J F, Kang C W, Fang F Z. Study on surface texture patterns for improving tribological performance of bioimplants. Surface and Coatings Technology, 2021, 422: 127567
26. Lancaster J G, Dowson D, Isaac G H, Fisher J. The wear of ultra-high molecular weight polyethylene sliding on metallic and ceramic counterfaces representative of current femoral surfaces in joint replacement. Proceedings of the Institution of Mechanical Engineers, Part H: Journal of Engineering in Medicine, 1997, 211(1): 17–24
27. Wang A, Polineni V K, Stark C, Dumbleton J H. Effect of femoral head surface roughness on the wear of ultrahigh molecular weight polyethylene acetabular cups. The Journal of Arthroplasty, 1998, 13(6): 615–620
28. Welghtman B, Light D. The effect of the surface finish of alumina and stainless steel on the wear rate of UHMW polyethylene. Biomaterials, 1986, 7(1): 20–24
29. Feng D, Shen M X, Peng X D, Meng X K. Surface roughness effect on the friction and wear behaviour of acrylonitrile–butadiene rubber (NBR) under oil lubrication. Tribology Letters, 2017, 65(1): 10
30. Shen G, Zhang J F, Melentiev R, Fang F Z. Study on tribological performance of groove-textured bioimplants. Journal of the Mechanical Behavior of Biomedical Materials, 2021, 119: 104514
31. Kovacı H, Seçer Y. Improved tribological performance of AISI 316L stainless steel by a combined surface treatment: surface texturing by selective laser melting and plasma nitriding. Surface and Coatings Technology, 2020, 400: 126178
32. Xi Y W, Kaper H J, Choi C H, Sharma P K. Tribological properties of microporous polydimethylsiloxane (PDMS) surfaces under physiological conditions. Journal of Colloid and Interface Science, 2020, 561: 220–230
33. Xi Y W, Sharma P K, Kaper H J, Choi C H. Tribological properties of micropored poly (2-hydroxyethyl methacrylate) hydrogels in a biomimetic aqueous environment. ACS Applied Materials & Interfaces, 2021, 13(35): 41473–41484
34. Choudhury D, Rebenda D, Sasaki S, Hekrle P, Vrbka M, Zou M. Enhanced lubricant film formation through micro-dimpled hard-on-hard artificial hip joint: an *in-situ* observation of dimple shape effects. Journal of the Mechanical Behavior of Biomedical Materials, 2018, 81: 120–129
35. Ito H, Kaneda K, Yuhta T, Nishimura I, Yasuda K, Matsuno T.

Reduction of polyethylene wear by concave dimples on the frictional surface in artificial hip joints. The Journal of Arthroplasty, 2000, 15(3): 332–338
36. Qiu M F, Chyr A, Sanders A P, Raeymaekers B. Designing prosthetic knee joints with bio-inspired bearing surfaces. Tribology International, 2014, 77: 106–110
37. Sadeghi M, Kharaziha M, Salimijazi H R, Tabesh E. Role of micro-dimple array geometry on the biological and tribological performance of Ti6Al4V for biomedical applications. Surface and Coatings Technology, 2019, 362: 282–292
38. Wei X F, Li W J, Liang B J, Li B L, Zhang J J, Zhang L S, Wang Z B. Surface modification of Co–Cr–Mo implant alloy by laser interference lithography. Tribology International, 2016, 97: 212–217
39. Pratap T, Patra K. Mechanical micro-texturing of Ti-6Al-4V surfaces for improved wettability and bio-tribological performances. Surface and Coatings Technology, 2018, 349: 71–81
40. Chyr A, Qiu M F, Speltz J W, Jacobsen R L, Sanders A P, Raeymaekers B. A patterned microtexture to reduce friction and increase longevity of prosthetic hip joints. Wear, 2014, 315(1–2): 51–57
41. Nečas D, Vrbka M, Rebenda D, Gallo J, Galandáková A, Wolfová L, Křupka I, Hartl M. *In situ* observation of lubricant film formation in THR considering real conformity: the effect of model synovial fluid composition. Tribology International, 2018, 117: 206–216
42. Roy T, Choudhury D, Ghosh S, Bin Mamat A, Pingguan-Murphy B. Improved friction and wear performance of micro dimpled ceramic-on-ceramic interface for hip joint arthroplasty. Ceramics International, 2015, 41(1): 681–690
43. Zhang H, Qin L G, Hua M, Dong G N, Chin K S. A tribological study of the petaloid surface texturing for Co–Cr–Mo alloy artificial joints. Applied Surface Science, 2015, 332: 557–564
44. Shen G, Zhang J F, Fang F Z. Study on the effect of hydrodynamic pressure on the tribological performance of textured bioimplants. Proceedings of the Institution of Mechanical Engineers, Part C: Journal of Mechanical Engineering Science, 2022, 236(6): 3135–3145
45. Pratap T, Patra K. Tribological performances of symmetrically micro-textured Ti-6Al-4V alloy for hip joint. International Journal of Mechanical Sciences, 2020, 182: 105736
46. Melentiev R, Fang F Z. Fabrication of micro-channels on Co–Cr–Mo joints by micro-abrasive jet direct writing. Journal of Manufacturing Processes, 2020, 56: 667–677
47. Longmore R B, Gardner D L. The surface structure of ageing human articular cartilage: a study by reflected light interference microscopy (RLIM). Journal of Anatomy, 1978, 126(Pt 2): 353–365
48. Melentiev R, Fang F Z. Tailoring of surface topography for tribological purposes by controlled solid particle impacts. Wear, 2020, 444–445: 203164
49. Kang C W, Liang F S, Shen G, Wu D X, Fang F Z. Study of micro-dimples fabricated on alumina-based ceramics using micro-abrasive jet machining. Journal of Materials Processing Technology, 2021, 297: 117181
50. Saikko V. Effect of contact area on the wear of ultrahigh molecular weight polyethylene in noncyclic pin-on-disk tests. Tribology International, 2017, 114: 84–87
51. Saikko V. Effect of lubricant protein concentration on the wear of ultra-high molecular weight polyethylene sliding against a CoCr counterface. Journal of Tribology, 2003, 125(3): 638–642
52. Shen G, Zhang J F, Fang F Z. *In vitro* evaluation of artificial joints: a comprehensive review. Advances in Manufacturing, 2019, 7(1): 1–14
53. Nečas D, Vrbka M, Marian M, Rothammer B, Tremmel S, Wartzack S, Galandáková A, Gallo J, Wimmer M A, Křupka I, Hartl M. Towards the understanding of lubrication mechanisms in total knee replacements—part I: experimental investigations. Tribology International, 2021, 156: 106874
54. Marian M, Orgeldinger C, Rothammer B, Nečas D, Vrbka M, Křupka I, Hartl M, Wimmer M A, Tremmel S, Wartzack S. Towards the understanding of lubrication mechanisms in total knee replacements—part II: numerical modeling. Tribology International, 2021, 156: 106809
55. Rothammer B, Marian M, Rummel F, Schroeder S, Uhler M, Kretzer J P, Tremmel S, Wartzack S. Rheological behavior of an artificial synovial fluid—influence of temperature, shear rate and pressure. Journal of the Mechanical Behavior of Biomedical Materials, 2021, 115: 104278
56. Marian M, Shah R, Gashi B, Zhang S, Bhavnani K, Wartzack S, Rosenkranz A. Exploring the lubrication mechanisms of synovial fluids for joint longevity—a perspective. Colloids and Surfaces B: Biointerfaces, 2021, 206: 111926
57. Lancaster J K. Abrasive wear of polymers. Wear, 1969, 14(4): 223–239
58. Xie Y, Williams J A. The prediction of friction and wear when a soft surface slides against a harder rough surface. Wear, 1996, 196(1–2): 21–34
59. Affatato S. Wear of orthopaedic implants and artificial joints. Woodhead Publishing, 2012
60. Jalali-Vahid D, Jagatia M, Jin Z M, Dowson D. Prediction of lubricating film thickness in UHMWPE hip joint replacements. Journal of Biomechanics, 2001, 34(2): 261–266
61. Wang A, Essner A, Stark C, Dumbleton J H. Comparison of the size and morphology of UHMWPE wear debris produced by a hip joint simulator under serum and water lubricated conditions. Biomaterials, 1996, 17(9): 865–871
62. Que L, Topoleski L D T, Parks N L. Surface roughness of retrieved CoCrMo alloy femoral components from PCA artificial total knee joints. Journal of Biomedical Materials Research, 2000, 53(1): 111–118
63. Caravia L, Dowson D, Fisher J, Jobbins B. The influence of bone and bone cement debris on counterface roughness in sliding wear tests of ultra-high molecular weight polyethylene on stainless steel. Proceedings of the Institution of Mechanical Engineers, Part H: Journal of Engineering in Medicine, 1990, 204(1): 65–70
64. Choudhury D, Vrbka M, Mamat A B, Stavness I, Roy C K, Mootanah R, Krupka I. The impact of surface and geometry on coefficient of friction of artificial hip joints. Journal of the Mechanical Behavior of Biomedical Materials, 2017, 72: 192–199